

Pairwise-additive models for atom-surface interaction potentials: An *ab initio* study of He-LiF

P. W. Fowler* and Jeremy M. Hutson

University Chemical Laboratory, Lensfield Road, Cambridge, CB2 1EW, England

(Received 7 October 1985)

Ab initio self-consistent-field calculations of the repulsive part of the He-F⁻ and He-Li⁺ interaction potentials are performed, together with coupled Hartree-Fock calculations of the dispersion coefficients determining the attractive part. The results are then used to construct an atom-surface potential for He-LiF, based on pairwise additivity of atom-ion forces. Ions in the crystal are simulated by performing calculations on a cluster consisting of an anion and its shell of nearest-neighbor cations, embedded in a point-charge lattice. Environments appropriate to ions in the bulk or at the surface can be constructed. Repulsion potentials between He atoms and in-crystal ions are found to be significantly weaker than those involving free ions. Anions at the surface are found to be slightly more polarizable than those in the bulk, but both are much less polarizable than free anions. Dispersion coefficients involving ions in different environments show similar trends. A model of the atom-surface potential is proposed, based on pairwise additivity but including corrections for induction energy, nonadditive dispersion forces, and dielectric screening effects. With semiempirical values of the dispersion coefficients based on the *ab initio* calculations, the resulting atom-surface potential has a well depth of 8.11 meV, compared with an experimental value of approximately 8.7 meV.

I. INTRODUCTION

Recent advances in experimental methods for observing the scattering of atoms from solid surfaces have led to a need for accurate atom-surface interaction potentials. There has been considerable interest in pairwise-additive models for such potentials, in which the atom-surface potential is written in the form

$$V(\mathbf{r}) = \sum_i V_i(\rho_i), \quad (1)$$

where the vector \mathbf{r} denotes the position of the adatom above the surface, and the sum runs over all atoms (or ions) in the solid. ρ_i is the distance from the adatom to atom i of the solid, and $V_i(\rho_i)$ is the appropriate pair potential. Pairwise-additive models have been applied to the scattering of He atoms from several surfaces; these include overlayers of Kr and Xe on substrates such as graphite and silver,¹⁻⁵ graphite itself,^{6,7} and ionic solids such as LiF.⁸⁻¹⁰

The formulation (1) is clearly approximate, and may be viewed in either of two ways. The pair potentials $V_i(\rho_i)$ may be assumed to be the same as the corresponding gas-phase pair potentials, which are independently known for systems such as rare-gas pairs; in this case, the corrections to Eq. (1) are due to many-body interactions. Alternatively, the $V_i(\rho_i)$ may be regarded as *effective* pair potentials, chosen to reproduce the atom-surface potential as well as possible, but not necessarily related to the gas-phase pair potentials. This latter viewpoint is certainly more appropriate for ionic solids, since ions in crystals are known to differ substantially from free ions.^{11,12}

Celli *et al.*¹⁰ have applied a pairwise-additive model to the He-LiF potential. They represented the atom-surface

potential as in Eq. (1), with an induction contribution due to the polarization of the He atom in the field of the ions

$$V(\mathbf{r}) = \sum_i V_i(\rho_i) + V^{\text{ind}}(\mathbf{r}). \quad (2)$$

The individual He-ion pair potentials were expressed in the semiempirical form

$$V(\rho) = A \exp(-b\rho) - \sum_{n=3} f_{2n}(\rho) C_{2n} \rho^{-2n}, \quad (3)$$

using the dispersion damping functions $f_{2n}(\rho)$ proposed by Tang and Toennies for gas-phase pair potentials¹³

$$f_{2n}(\rho) = 1 - \sum_{k=0}^{2n} [(b\rho)^k / k!] \exp(-b\rho). \quad (4)$$

Celli *et al.* took repulsive parameters A and b from first-order self-consistent-field (SCF) calculations on gas-phase He-Li⁺ and He-F⁻ pairs,¹⁴ and truncated the dispersion series after the first term ($2n=6$). The He-Li⁺ C_6 coefficient was taken from Dalgarno and Davison,¹⁵ and the He-F⁻ C_6 coefficient was optimized so that the resulting potential reproduced the experimental He-LiF bound-state energies of Derry *et al.*¹⁶ Celli *et al.* were quite successful in reproducing the existing scattering data with this potential, but it has certain theoretical drawbacks; its long-range C_3 coefficient is considerably larger than suggested by other considerations,¹⁷⁻¹⁹ and the absence of dispersion coefficients for $2n > 6$ is physically implausible. Celli *et al.* experimented with such higher-order terms, but found that they worsened the fit to the bound-state energies.

The application of pairwise-additive models to ionic solids raises several questions.

(1) How similar are He-ion repulsive potentials for free and in-crystal ions? Is it reasonable to use repulsive potentials calculated for free ions when constructing atom-surface potentials?

(2) How similar are He-ion dispersion coefficients for free and in-crystal ions? Are *surface* ions similar to *bulk* ions in this respect?

(3) Are the He-ion dispersion forces significantly modified by dielectric screening effects? How are such screening effects related to many-body interactions?

The purpose of the present paper is to describe *ab initio* calculations on ions in crystals which enable us to address these questions. It will be shown that in-crystal ions and free ions differ very significantly, but that (at least for LiF) surface ions are quite similar to bulk ions. The *ab initio* results will then be used to construct a He-LiF interaction potential, for comparison with the experimental bound-state energies.¹⁶ Future work will deal with the fitting, to molecular-beam scattering data, of a gas-surface potential obeying the theoretical constraints.

The calculations described below also throw light on the extent to which the polarizabilities of surface ions differ from those of bulk and free ions. Enhanced polarizabilities at the surface have been proposed in an attempt to explain surface phonon frequencies,^{20,21} and our calculations provide some support for this.

II. SHORT-RANGE REPULSIVE POTENTIAL

In this section we consider the repulsive part of the interaction potential between He and the ions F^- and Li^+ . The method used is an *ab initio* supermolecule calculation at the SCF level, with corrections for basis-set superposition error (BSSE) and induction energy. Attractive contributions from dispersion forces are, of course, not present in an SCF calculation.

It is known that anions in crystals are strongly affected by their environment,¹² whereas cations are relatively insensitive to it.²² Thus the He- F^- potentials for free and in-crystal F^- ions may be expected to differ considerably, while the corresponding potentials for He- Li^+ (for free and in-crystal Li^+ ions) will be quite similar. In order to study the effect of the environment, the repulsive potential for He- F^- has been calculated both for a free F^- ion and for an F^- ion embedded in a simulation of the (100) face of an LiF crystal.

Previous work has shown that an anion in a crystal is smaller,¹¹ less polarizable,¹² and more strongly bound²³ than the corresponding free anion. Two physical factors account for most of this effect:¹² electrostatic interaction with the lattice of ions, and overlap compression by the charge clouds of the nearest neighbors. A good simulation of the crystalline environment in the bulk can be achieved by calculations on a cluster where the anion is surrounded by a shell of nearest-neighbor cations, and more distant ions are represented by a finite lattice of point charges.^{12,22,24} Such calculations give, for example, excellent agreement with experiment for the static polarizability of F^- in LiF. Charge-transfer effects on the ionic size and polarizability are small.¹² The qualitative picture

which emerges is that an ion deep in the body of a crystal is effectively confined in a spherical box (or potential well) due to the presence of the neighboring ions.

For an ion at the surface of a crystal, this picture is somewhat modified. Such an ion is in an anisotropic effective potential, subject to an electric field normal to the surface, and free from overlap compression from above. We have constructed a simulation of this environment for an idealized (100) face of LiF by placing a cluster consisting of one F^- ion and its five nearest-neighbor Li^+ ions in a $7 \times 7 \times 4$ lattice of point charges, as shown in Fig. 1. This approach is somewhat similar to that used by Colbourn and Mackrodt²⁵ in studies of the chemisorption of H_2 and CO on MgO. The charges on the faces of the point-charge lattice in the interior of the crystal were scaled to give overall electrical neutrality. An Li-F internuclear distance of $3.7965a_0$, appropriate to the bulk, was retained, so that possible surface relaxation and rumpling^{26,27} were ignored. As in the calculations on bulk ions, this model includes all electrostatic effects and compression of the anion by overlap with the nearest-neighbor cations, but neglects any effects due to overlap of different anions; the neglected effects are believed to be small for LiF, since the calculations on bulk ions gave good agreement with empirical in-crystal polarizabilities.¹²

The Gaussian basis set used here for the $(F^-)(Li^+)_5$ cluster was taken from Ref. 12. The $[12s\ 8p\ 5d]$ F^- basis set gives a polarizability near the Hartree-Fock limit for the free ion, while the highly contracted $(10s\ 5p) \rightarrow [1s\ 1p]$ Li^+ basis set gives a near-Hartree-Fock energy, polarizability, and charge density for Li^+ , but is small enough for use in a large cluster calculation. In the same manner, a basis set for He was chosen by contracting a $10s$ set²⁸ and a polarization $8p$ set (with the six most diffuse s exponents plus 0.07, 0.035) to $[1s\ 1p]$. Again, the energy ($-2.86167E_h$) and polarizability ($1.3219a_0^3$) in this compact basis are of essentially Hartree-Fock quality.

Using this approach, calculations of the total SCF energy were carried out for geometries in which a He atom lies directly above the F^- site of the cluster. He- F^- distances of $\rho = 3.75a_0$, $4.125a_0$, and $4.5a_0$ were considered. Subtracting the energy of the isolated $[1s\ 2p]$ He atom and of the $(F^-)(Li^+)_5$ cluster in the lattice from the super-

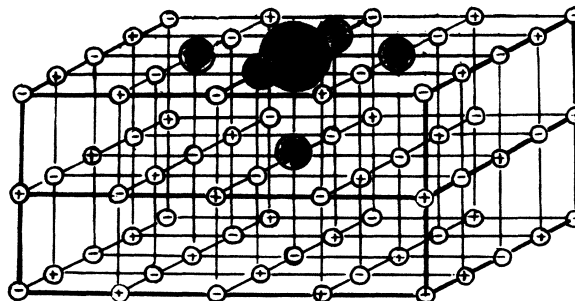


FIG. 1. Schematic diagram showing an $(F^-)(Li^+)_5$ cluster embedded in the surface of a point-charge lattice. The point-charge lattice used in the actual calculation was $7 \times 7 \times 4$, instead of the $5 \times 5 \times 3$ lattice shown here.

TABLE I. Repulsive energy of interaction of a He atom with a surface F^- ion, calculated at the SCF level. Units of energy are $10^{-5}E_h$. The symbols used are explained in the text. The final energies ΔE^{rep} were fitted to $A \exp(-bR)$ with $A = 19.258E_h$ and $b = 1.9676a_0^{-1}$.

R/a_0	ΔE^{uncorr}	ΔE^{BSSE}	ΔE^{ind}	ΔE^{He-Li}	ΔE^{rep}
3.75	1171.0	2.2	-33.3	3.7	1202.8
4.125	560.5	2.5	-13.8	1.7	575.0
4.5	267.8	2.3	-5.7	0.8	275.0

molecule energy, the interaction energy ΔE^{uncorr} is obtained, as shown in Table I.

In addition to the desired He- F^- repulsion energy, ΔE^{uncorr} contains three contributions that must be removed. First, it contains basis-set superposition error, arising from the lowering of the fragment energies in the larger basis of the supermolecule. This can be removed by the counterpoise technique,²⁹ in which the energy of each subsystem is separately calculated in the supermolecule basis. This correction is listed in Table I as ΔE^{BSSE} .

A second, physical contribution to ΔE^{uncorr} is the attractive induction energy, mainly arising from polarization of the He atom in the field of the crystal. We remove this term by calculating the energy of a $[1s\ 1p]$ He atom at a distance ρ above a complete point-charge lattice [i.e., a lattice where the ions $(F^-)(Li^+)_5$ are replaced by point charges]. The resulting induction contribution is denoted ΔE^{ind} in Table I.

Finally, the repulsive energy of interaction of the He atom with the five Li^+ ions in the cluster must be subtracted. A repulsive potential was calculated for He and an Li^+ ion embedded in a point-charge lattice (both in the $[1s\ 1p]$ bases), yielding the results shown in Table II; it may be noted that the induction energies are somewhat different from those of Table I.³⁰ After subtracting out the induction contribution, the He- Li^+ potential was fitted to the single exponential form

$$V(\rho) = A \exp(-b\rho). \quad (5)$$

BSSE corrections for He- Li^+ were found to be negligible. The sum of He- Li^+ energies calculated with this function is listed under ΔE^{He-Li} for each cluster geometry in Table I.

The final energy ΔE^{He-F} is found from

$$\Delta E^{He-F} = \Delta E^{uncorr} + \Delta E^{BSSE} - \Delta E^{ind} - \Delta E^{He-Li} \quad (6)$$

and fitted to the functional form (5). It may be noted that, at least over this range of ρ , the simple exponential

TABLE II. Repulsive energy of interaction of a He atom with a surface Li^+ ion, calculated at the SCF level. Units of energy are $10^{-5}E_h$. The symbols used are explained in the text. The final energies ΔE^{rep} were fitted to $A \exp(-bR)$ with $A = 35.905E_h$ and $b = 2.8425a_0^{-1}$.

R/a_0	ΔE^{uncorr}	ΔE^{ind}	ΔE^{rep}
3.25	275.4	-72.3	347.8
3.50	129.2	-42.8	172.0
3.75	59.7	-24.9	84.6
4.50	5.2	-4.7	10.0

fit is very good: the geometric mean of the energies for $\rho = 3.75$ and $4.5a_0$ is $(575 \times 10^{-5})E_h$, exactly equal to the *ab initio* result for $\rho = 4.125a_0$.

Similar sets of calculations were carried out for the interaction of He with free F^- and Li^+ ions; the results are shown in Tables III and IV. Again, it may be noted that the calculated point-charge induction energies are somewhat different for He- F^- and He- Li^+ .³⁰ In addition, the point-charge model neglects terms arising from the interaction of the *induced* moments on He with the polarizabilities of the ion, which are not negligible for the free-ion interaction. The leading contribution may be estimated to be of order $\alpha_{ion}\alpha_{He}^2/\rho^{10}$, which would add about $(3 \times 10^{-5})E_h$ to the calculated He-free F^- repulsion at $\rho = 3.75a_0$ and about $(0.5 \times 10^{-5})E_h$ at $\rho = 4.5a_0$.

The repulsive potentials for He- F^- (surface) and He- F^- (free) are shown in Tables I and III and Fig. 2, and it may be seen that they are significantly different (note the logarithmic scale). At separations greater than about $3.20a_0$ (1.70 Å), the free F^- ion is more repulsive, and the repulsion has a longer "tail." This is compatible with the diffuse nature of the free anion compared to the more compact in-crystal species. Our free-anion potential is, however, much *less* repulsive than the first-order SCF potential¹⁴ used in Ref. 10 (also shown in Fig. 2), for which $A = 160.2E_h$ and $b = 2.347a_0^{-1}$; at $\rho = 3.75a_0$, the present potential is almost a factor of 2 weaker. It is known that the first-order SCF procedure overestimates repulsion,³¹ because it neglects relaxation of the charge densities of the interacting systems, and for large polarizable anions such as F^- this error will be particularly important. Thus we believe that our SCF results for the He-free F^- potential are closer to the Hartree-Fock limit than those of Ref. 14. However, it should be noted that correlation increases the polarizability of free F^- by 40% or more,¹² and there is a corresponding increase in the ionic size; thus the SCF potential, even at the Hartree-Fock limit, is probably an underestimate of the full repulsive potential for the *free*

TABLE III. Repulsive energy of interaction of a He atom with a free F^- ion, calculated at the SCF level. Units of energy are $10^{-5}E_h$. The symbols used are explained in the text. The final energies ΔE^{rep} were fitted to $A \exp(-bR)$ with $A = 9.249E_h$ and $b = 1.7392a_0^{-1}$.

R/a_0	ΔE^{uncorr}	ΔE^{BSSE}	ΔE^{ind}	ΔE^{rep}
3.75	1042.8	0.1	-321.2	1364.1
4.125	483.0	0.1	-221.4	704.5
4.5	212.7	0.1	-157.4	370.1

TABLE IV. Repulsive energy of interaction of a He atom with a free Li^+ ion, calculated at the SCF level. Units of energy are $10^{-3}E_h$. The symbols used are explained in the text. The final energies ΔE^{rep} were fitted to $A \exp(-bR)$ with $A = 43.909E_h$ and $b = 2.8066a_0^{-1}$.

R/a_0	ΔE^{uncorr}	ΔE^{ind}	ΔE^{rep}
3.25	-94.7	-566.7	472.0
3.50	-193.7	-433.3	239.6
3.75	-214.1	-334.2	120.1
4.50	-149.4	-163.6	14.2

anion. In contrast, the *in-crystal* anion has a much smaller radial correlation,^{12,22} and the SCF results are likely to give a good estimate of the true repulsion.

The question also arises whether the repulsion due to a surface F^- ion is significantly anisotropic. In order to investigate this, we have performed SCF calculations for a variety of orientations of the approach of a He atom to a surface F^- ion, and the results are listed in Table V. These calculations use the same basis sets as for the normal approach, except that the contracted $1p$ functions on the Li^+ ions were omitted. As may be seen by comparing the 0° calculations of Table V with those of Table I, the larger and smaller basis sets give very similar repulsion energies. For $\theta \leq 20^\circ$, the SCF repulsion energies due to the F^- ion are within 1% of those for $\theta = 0^\circ$, and the repulsion anisotropy may thus be neglected. This is in direct contradiction to the results of Miglio *et al.*,^{32,33} who predicted substantial quadrupolar distortion of surface ions due to the electric field gradient at a surface site. As will be discussed below, their calculation neglected both the effect of the crystalline environment on the quadrupole polarizability and the overlap distortion by neighboring ions, and both these effects reduce the extent of the quadrupole distortion.

The repulsive potential for He- Li^+ (crystal) is also weaker than that for He- Li^+ (free). In this case the differences are less important to the He-LiF atom-surface potential since, even for approach of a He atom directly over an Li^+ ion, the He-LiF repulsion potential is dominated by He- F^- interactions.

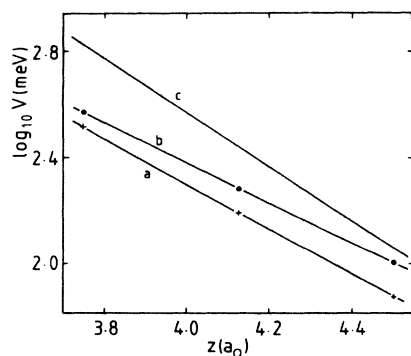


FIG. 2. Calculated repulsion potentials for He- F^- : curve *a*, SCF He-surface F^- potential; curve *b*, SCF He-free F^- potential; curve *c*, "first-order" SCF He- F^- potential of Ref. 14.

In summary, therefore, potential parameters appropriate to the scattering of He from LiF can be calculated only if the effect of the crystalline-environment on the F^- ion is included. Repulsion potentials for the free ion are not only difficult to calculate accurately but are inappropriate for use in constructing atom-surface potentials.

III. PROPERTIES OF SURFACE IONS

In this section we consider how the properties of an F^- ion at the surface of LiF may be calculated, how they compare with those of the ion in the bulk, and what they tell us about the interaction potential for He-LiF. The properties considered are of two types: first-order properties such as the dipole and higher moments of the charge density, and second-order properties such as the frequency-dependent polarizability $\alpha(i\omega)$. The attractive part of the pair potential for He- F^- involves these properties since the permanent multipole moments contribute to the induction energy, and the polarizability at imaginary frequency determines C_6 dispersion coefficients.

As in previous work on ions in the bulk,^{12,22} calculations are performed in two stages in order to separate the physical factors responsible for the difference between free and in-crystal ions. In the first stage, denoted XTAL in Ref. 12, an F^- ion is placed in a point-charge lattice to represent the effect of the Coulomb electrostatic interaction between an ion and its neighbors in the lattice. As in Sec. II, a $7 \times 7 \times 4$ slab of the lattice of LiF was used, with F^- at the center of the top layer. SCF and coupled Hartree-Fock (CHF) calculations³⁴ with the $[12s8p5d]$ basis of Ref. 12 gave the results shown in Table VI. The z direction is the outward normal from the surface, and x and y lie in the surface plane.

In the second stage, overlap effects are simulated by using "real" Li^+ neighbors complete with basis functions and electrons, the whole cluster being embedded in the $7 \times 7 \times 4$ point-charge lattice (see Fig. 1). A calculation of this type is denoted CLUS in Ref. 12. For use in pairwise-additive potential models, the properties of the cluster must be partitioned into contributions from the different ions. This was done differently for first-order and second-order properties. For first-order properties, moments of the charge density were calculated for a cage $(\text{Li}^+)_5$ in the lattice, with a negative point charge replacing the F^- ion. The moments appropriate to the in-surface F^- ion were then obtained by subtraction. BSSE corrections to this simple procedure were calculated, but were found to be negligible. For polarizabilities, the six lowest occupied molecular orbitals were "frozen" in the CHF calculation, thus allowing the valence electrons of F^- but not of Li^+ to polarize. This is not the same as the partitioning used for bulk ions in Ref. 12, where polarizabilities, BSSE effects, and dipole-induced-dipole corrections were removed explicitly from the calculated total polarizability of the cluster.

A. Static properties

Table VI reports the calculated moments and static polarizability of the F^- ion in five different environments: the free ion, the electrostatically compressed XTAL ion at

TABLE V. Repulsive energy of interaction of a He atom with a surface F^- ion, calculated at the SCF level, for various directions of approach. The angle θ is measured in the plane of the F^- ion and a nearest-neighbor cation. The basis set is slightly different from that used in Table I (see text), and the column $\Delta E^{\text{He-Li}}$ refers to the He-Li⁺ repulsion in the new basis. Units of energy are $10^{-5}E_h$.

θ (deg)	ΔE^{uncorr}	ΔE^{BSSE}	ΔE^{ind}	$\Delta E^{\text{He-Li}}$	ΔE^{rep}
(a) Angle dependence for $R = 4.125a_0$					
0	567.4	2.5	-13.8	2.0	581.7
10	567.9	3.3	-13.4	3.3	581.3
20	571.9	5.0	-13.7	10.9	579.6
30	595.6	6.9	-21.5	51.7	572.3
(b) Angle dependence for $R = 3.75a_0$					
0	1179.6	2.0	-33.3	4.3	1210.5
20	1192.3	6.2	-33.6	20.8	1211.4

the surface and in the bulk, and the electrostatically and overlap compressed CLUS ion at the surface and in the bulk.

On the surface of the crystal, F^- occupies a site of C_{4v} symmetry, which is lower than the symmetry of a site deep within the crystal (O_h). The surface ion therefore has permanent dipole and quadrupole moments and an axially symmetric polarizability tensor. At the purely electrostatic XTAL level, the dipole moment of F^- is $0.1127ea_0$; the electric field of the point-charge lattice would, if uniform, induce a dipole moment of about $0.15ea_0$. The positive sign implies that, on average, the electrons are pulled below the surface plane by the crystal field. However, when overlap from nearest-neighbor cations is included in the calculation, the dipole moment is reduced to only $0.0241ea_0$, as the overlap compression from the Li^+ directly beneath the F^- ion pushes electrons in the opposite direction.

In the point-charge lattice, the surface F^- ion has a positive quadrupole moment of $0.1153ea_0^2$, indicating an oblate charge cloud where the expectation value $\langle x^2 \rangle = \langle y^2 \rangle$ is about 2% greater than $\langle z^2 \rangle$. As the second moments $Q_{\alpha\beta}$ show, the surface ion in the XTAL calculation is smaller than the free ion, and is almost identical in size to the XTAL ion within the crystal (although the electrons are now anisotropically distributed). On adding overlap effects, the anisotropy is reduced, this time because the density is compressed more along the x and y directions than along the z direction. At this level

of calculation, the ion at the surface has a slightly larger radius (about 1% in $\langle r^2 \rangle$) than the bulk ion.

Our calculated quadrupole moments may be compared with the value $\Theta_z = 0.84ea_0^2$, estimated by Miglio *et al.*^{32,33} by using the quadrupole polarizability of the free anion to describe the response of the ion to the field gradient at a surface site. This is a poor approximation for several reasons. First, the quadrupole polarizability of the bulk F^- ion is reduced by a factor of about 4 from the free-ion value,³⁵ and our experience with dipole polarizabilities suggests that this smaller value will be the one appropriate to the surface ion; secondly, a multipole expansion of the field is likely to misrepresent the electrostatic effects of the first shell of neighbors;³⁶ and thirdly, overlap effects act to reduce the electrostatically induced moment. The calculations given in Refs. 32 and 33 thus drastically overestimate the quadrupolar distortion.

The polarizability behaves much as expected from $\langle x^2 \rangle$, $\langle y^2 \rangle$, and $\langle z^2 \rangle$. At the XTAL level, we find that the polarizability normal to the surface is smaller than that parallel to the surface. The field which pulls electrons down into the solid has the effect of restricting motion along the field direction, so that α_z is reduced from the bulk XTAL value. The trace of the polarizability tensor is, however, larger at the surface than in the bulk, because of the greater freedom of the electron density above the surface plane.

In the full cluster calculation, the surface ion still has a greater mean polarizability than its bulk counterpart (by

TABLE VI. Properties of the F^- ion in different environments, obtained from CHF calculations. μ is the dipole moment, Θ the quadrupole moment (Ref. 39), and Q the second moment of the charge density. The z axis is the outward normal from the surface plane. Atomic units are used throughout.

	XTAL			CLUS	
	Free	Surface	Bulk	Surface	Bulk
μ_z		0.1127		0.0241	
Θ_z		0.1153		0.0204	
Q_{xx}	-5.328	-5.092	-5.014	-4.780	-4.716
Q_{zz}	-5.328	-4.976	-5.014	-4.760	-4.716
α_{xx}	10.654	7.833	7.300	5.741	5.40
α_{zz}	10.654	6.997	7.300	5.893	5.40

about 7%), but now the sign of the anisotropy is reversed, with $\alpha_{zz} > \alpha_{xx}$, presumably because overlap effects in α_{zz} counteract the effect of the electrostatic field and the outer reaches of the charge density above the surface plane are less restricted than in the bulk.

Both bulk and surface ions have polarizabilities almost a factor of 2 smaller than the free ion,¹² even at the CHF level. It is known that correlation effects enhance the polarizability of the free F^- ion by at least 40%,¹² but that they contribute much less for in-crystal ions; for the bulk (CLUS) F^- ion in LiF, for example, the correlation contribution is only about 15%.²² The difference between the true polarizabilities of free and in-crystal (bulk and surface) F^- ions will thus be even greater than shown in Table VI.

Overall, the surface F^- ion is similar in properties to the bulk ion. It is slightly larger, a few percent more polarizable, and is slightly anisotropic. The small permanent moments modify the field experienced by an approaching atom only very slightly, and do not contribute significantly to the atom-surface induction energy. Because of its small polarizability and general insensitivity to the crystalline environment,²² an Li^+ ion on the surface is expected to be even more similar to a bulk ion than is the case for F^- .

B. Dispersion coefficients

In addition to the static properties detailed in Table VI, the frequency-dependent polarizability of the surface F^- ion was calculated at 16 imaginary frequencies $i\omega$. These quantities have already been calculated for the free F^- ion, XTAL and CLUS bulk F^- ions, and the Li^+ ion,³⁷ using the same basis sets as in the present work. The polarizability of He was calculated in the full uncontracted (10s8p) basis at the same frequencies. All calculations were at the CHF level, and followed Ref. 37 in detail.

The importance of the quantities $\alpha(i\omega)$ lies in their relation to dispersion coefficients. The dispersion coefficient C_6 between two species A and B is given by

$$C_6(A,B) = (3/\pi) \int_0^\infty \alpha_A(i\omega)\alpha_B(i\omega)d\omega. \quad (7)$$

In the present work, $\alpha(i\omega)$ was calculated at 16 imaginary frequencies, and the integrals were evaluated using transformed Gauss-Legendre quadrature as described in Ref. 38, with a scaling parameter $\omega_0 = 0.2E_h$; the results for $C_6(He-Li^+)$ and $C_6(He-F^-)$ in various environments are given in the "CHF" column of Table VII. Because of the anisotropy of the surface F^- ion, there are two independent components of the corresponding $C_6(He-F^-)$ coefficient, but these differ by only 0.5%. As expected from the static polarizabilities, $C_6(He-F^-)$ is larger for a surface ion than for one in the bulk, but both values are very much smaller than for a free F^- ion.

The second term in the dispersion series, the dipole-quadrupole coefficient C_8 , may also be evaluated from CHF calculations. It is given by

$$C_8(A,B) = (15/\pi) \int_0^\infty [\alpha_A(i\omega)C_B(i\omega) + C_A(i\omega)\alpha_B(i\omega)]d\omega, \quad (8)$$

where the fourth-rank tensor C is the quadrupole polarizability.³⁹ The dynamic C tensor has been evaluated for Li^+ and in-crystal (bulk CLUS) F^- ions by Fowler and Pyper,³⁵ and yields coefficients $C_8(He-Li^+) = 1.98$ a.u. and $C_8(He-F^-) = 71.7$ a.u.; it may be noted that these are in quite good agreement with estimates using the approximate expression of Starkschall and Gordon,⁴⁰

$$C_8(A,B) \approx \frac{3}{2} C_6(A,B) \left[\frac{\langle r^4 \rangle_A}{\langle r^2 \rangle_A} + \frac{\langle r^4 \rangle_B}{\langle r^2 \rangle_B} \right], \quad (9)$$

which yields 1.96 and 64.8 a.u. for the $He-Li^+$ and $He-F^-$ C_8 coefficients, respectively, using the CHF values of the corresponding C_6 coefficients.

IV. CONSTRUCTION OF A POTENTIAL MODEL

A. Pairwise summation

When performing scattering calculations, the atom-surface potential is usually represented as a Fourier series

$$V(\mathbf{r}) = \sum_G V_G(z) \exp(i\mathbf{G} \cdot \mathbf{R}), \quad (10)$$

where \mathbf{G} is a two-dimensional reciprocal-lattice vector in the surface plane, and \mathbf{R} is the projection of \mathbf{r} onto the plane. In the present work, the surface unit cell for LiF is taken to be a square of side a , with four F^- ions at the corners and an Li^+ ion at the center. The Li-F nearest-neighbor distance and the interplanar separation normal to the surface are thus $a/\sqrt{2}$. For pairwise-additive potentials, Steele⁴¹ has shown that a summation over a layer of atoms may be rewritten as an integral over the surface plane, and that the Fourier components may be written

$$V_G(z) = (2\pi/A) \int_0^\infty V(\rho, \theta) J_0(g t) t dt, \quad (11)$$

where $A = a^2$ is the area of the surface unit cell; J_0 is the Bessel function of order 0; $g = |\mathbf{G}|$; and the coordinates ρ , θ , and t are as shown in Fig. 3(a). Steele's treatment is valid provided the pair potential can be written as a function of ρ and θ only.

For inverse power potentials, $V(\rho, \theta) = -C_{2n}\rho^{-2n}$, Eq. (11) may be integrated analytically.⁴¹ This remains true even for anisotropic potentials, if the anisotropy is of the form $\cos^{2m}\theta$. The general result for $V(\rho, \theta) = -C_{2n}^{2m}\rho^{-2n}\cos^{2m}\theta$ is

$$V_{00}(z) = \frac{-\pi C_{2n}^{2m}}{A(n+m-1)z^{2n-2}}, \quad (12)$$

$$V_G(z) = \frac{-2\pi}{A} \frac{C_{2n}^{2m} z^{2m}}{(n+m-1)!} \left[\frac{g}{2z} \right]^{n+m-1} K_{n+m-1}(gz) \quad \text{for } \mathbf{G} \neq 0, \quad (13)$$

where K_n is a modified spherical Bessel function of the second kind. Thus an anisotropic pair potential yields a longer-range corrugation than an isotropic potential, but contributes to the same inverse power term in the surface-averaged potential. For an anisotropic C_6 term of the type discussed above for the surface layer, it may be noted that the effective isotropic coefficient [which gives

TABLE VII. Calculated dispersion coefficients for He-LiF. The SCF coefficients involving F^- ions are from CLUS calculations at the CHF level, and the semiempirical values use the model of Ref. 19. Values within parentheses in the CHF column are obtained by scaling, rather than by direct calculation. All values are in atomic units.

	CHF	Semiempirical
$C_6(\text{He, free } F^-)$	7.176	
$C_6(\text{He, Li}^+)$	0.291	0.295
$C_8(\text{He, Li}^+)$	1.98	2.01
$C_6(\text{He, bulk } F^-)$	5.160	5.773
$C_8(\text{He, bulk } F^-)$	71.7	80.2
$C_6^{xx}(\text{He, surface } F^-)$	5.350	6.036
$C_8^{xx}(\text{He, surface } F^-)$	(74.3)	83.9
$C_6^z(\text{He, surface } F^-)$	5.368	6.151
$C_8^z(\text{He, surface } F^-)$	(74.6)	85.5
$C_3(\text{He, LiF})$	0.02428	0.02675
$C_3^{(0)}(\text{He, LiF})$	0.02608	0.02903
L	0.9310	0.9215
$C_6^{\text{eff}}(\text{He, Li}^+)$	(0.271)	0.272
$C_8^{\text{eff}}(\text{He, Li}^+)$	(1.84)	1.85
$C_6^{\text{eff}}(\text{He, bulk } F^-)$	(4.804)	5.320
$C_8^{\text{eff}}(\text{He, bulk } F^-)$	(66.8)	73.9
$\nu(\text{He, surface } F^-, \text{ surface } F^-)$	21.4	28.2
$\nu(\text{He, surface } F^-, \text{ Li}^+)$	0.93	1.09
$\nu(\text{He, Li}^+, \text{ Li}^+)$	0.047	0.049
$C_{s2}(\text{He, LiF, surface } F^-)$	0.268	0.384
$C_{s2}(\text{He, LiF, Li}^+)$	0.0108	0.0139

the correct long-range term in $V_{00}(z)$ is

$$C_6^{\text{iso}} = \frac{1}{3}(C_6^{xx} + 2C_6^z). \quad (14)$$

This is *not* the usual isotropic average of the C_6 tensor, because the integral (11) emphasizes the contribution from values of θ close to zero. Equations (12) and (13) do not hold exactly when the dispersion forces include damping corrections, but they remain qualitatively useful.

B. Nonadditivity and dielectric screening

The dispersion forces between an atom and an ionic solid are not strictly pairwise additive. The fluctuating dipoles on different ions in the solid interfere with one another, and this interference modifies the dispersion interaction. This might, in principle, be treated by summing an n -body series

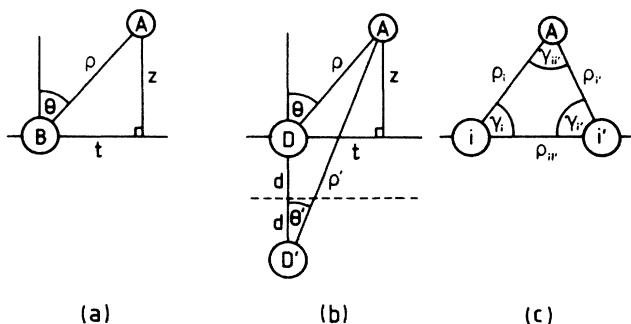


FIG. 3. Coordinate systems used for atom-surface systems: (a) for pairwise-additive terms; (b) for surface-mediated dispersion forces; (c) for the Axilrod-Teller triple-dipole term.

$$V(\mathbf{r}) = \sum_i V_i(\rho_i) + \sum_{ii'} V_{ii'}^{(3)}(\rho_i, \rho_{ii'}) + \dots, \quad (15)$$

where the summation run over all the ions in the solid. However, in practice, not enough is known about the n -body potentials, and the nonadditive terms are very expensive to evaluate, since they involve multiple summations over a three-dimensional lattice.

An alternative approach, which is equivalent at long range, is to treat the solid as a macroscopic polarizable dielectric.¹⁹ For a solid with a cubic crystal structure, the dielectric constant is given by the Clausius-Mossotti equation

$$\frac{\epsilon - 1}{\epsilon + 2} = \frac{4\pi}{3V} \sum_a \alpha_a, \quad (16)$$

where the index a runs over the ions in a (three-dimensional) unit cell of volume V , and α_a is an effective ionic polarizability. The factor $\epsilon + 2$ in the denominator arises from the Lorentz correction to the local field, and takes account of the field at a central ion due to dipolar polarization of all other ions in the solid. The long-range atom-surface dispersion coefficient C_3 may be expressed in terms of $\epsilon(i\omega)$ using the Lifshitz formula⁴²

$$C_3 = \frac{1}{4\pi} \int_0^\infty \alpha(i\omega) \left[\frac{\epsilon(i\omega) - 1}{\epsilon(i\omega) + 1} \right] d\omega. \quad (17)$$

Thus the C_3 coefficient may be evaluated directly from $\alpha(i\omega)$ functions for the adatom and for the ions in the solid. Note that it is the polarizabilities of bulk ions, *not* surface ions, which contribute to the C_3 coefficient; a modification of the polarizabilities at the surface can have important effects on the potential, but it appears as a term

of the form $C_4 z^{-4}$ and does not contribute to the C_3 coefficient. The value of C_3 obtained from Eq. (17) is *not* the same as that obtained assuming pairwise additivity, which is

$$C_3^{(0)} = (\pi/6V) \sum_a C_6(A, a). \quad (18)$$

The difference arises because the Clausius-Mossotti equation implicitly takes account of n -body effects (dielectric screening effects), which are neglected in the pairwise sum.

The Lorentz local-field correction is strictly valid only for ions deep inside the crystal. It is difficult to see how to generalize this approach to ions near the surface. However, when constructing a pairwise-additive model for the atom-surface potential, it seems reasonable to modify the dispersion coefficients for all ions *beneath the surface layer* to reproduce the correct limiting behavior. Thus we model the screening by writing

$$C_{2n}^{\text{eff}}(A, a) = LC_{2n}(A, a), \quad (19)$$

where

$$L = C_3/C_3^{(0)}. \quad (20)$$

This modification has little effect on the corrugation, which is almost entirely due to the surface layer.

For the surface layer itself, such an *ad hoc* scaling of the many-body forces is both less justified and more dangerous, and a more-detailed treatment is desirable. Many-body forces involving the surface layer may be divided into two categories:

- (1) Terms in which all the ions involved are in the surface layer.
- (2) Terms in which one or more of the ions involved is in the bulk.

These two contributions may be treated separately. The nonadditive terms within the surface layer may be approximated by the Axilrod-Teller triple-dipole expression

$$V_{ii'}^{(3)}(\rho_i, \rho_{i'}, \rho_{ii'}) = v(A, i, i') \frac{1 + 3 \cos \gamma_i \cos \gamma_{i'} \cos \gamma_{ii'}}{(\rho_i \rho_{i'} \rho_{ii'})^3}, \quad (21)$$

where the summation now runs over the ions in the surface layer only, the lengths and angles are as shown in Fig. 3(c), and

$$v(A, i, i') = (3/\pi) \int_0^\infty \alpha_A(i\omega) \alpha_i(i\omega) \alpha_{i'}(i\omega) d\omega. \quad (22)$$

Nonadditive terms involving ions beneath the surface layer may conveniently be taken into account using McLachlan's theory of surface-mediated dispersion forces between adatoms,⁴³ treating the surface layer as a layer of adatoms, and taking the "bulk" solid to start at the second layer. For two atoms A and D above the surface of a dielectric, McLachlan showed that the leading terms in the dispersion energy are

$$\begin{aligned} V^{AD}(\rho, \theta) = & -C_6(\rho)^{-6} \\ & + C_{s1} [2 - 3 \cos(2\theta) - 3 \cos(2\theta')] (\rho\rho')^{-3} \\ & - C_{s2}(\rho')^{-6}, \end{aligned} \quad (23)$$

where the coordinates ρ , ρ' , θ , and θ' are defined in Fig. 3(b). The coefficients C_{s1} and C_{s2} are given by

$$C_{s1}(A, BC, D) = \frac{3}{\pi} \int_0^\infty \alpha_A(i\omega) \left[\frac{\epsilon(i\omega) - 1}{\epsilon(i\omega) + 1} \right] \alpha_D(i\omega) d\omega, \quad (24)$$

$$C_{s2}(A, BC, D) = \frac{3}{\pi} \int_0^\infty \alpha_A(i\omega) \left[\frac{\epsilon(i\omega) - 1}{\epsilon(i\omega) + 1} \right]^2 \alpha_D(i\omega) d\omega. \quad (25)$$

The summation of this expression over a complete layer of surface ions D may be performed analytically using Steele's method,⁴¹ as described in the Appendix. For the surface-average potential $V_{00}(z)$, it turns out that the contribution from the C_{s1} term is identically zero, while the C_{s2} term contributes an attractive term of the form

$$-(\pi/2A)C_{s2}/(z + 2d)^4, \quad (26)$$

where d is the distance of the surface ions from the image plane, which may reasonably be taken to be half the interplanar separation. The contributions of the nonadditive terms to the corrugation of the potential are very small, and have been neglected in the present work.

C. Form of atom-surface potential

The final expression obtained for the atom-surface potential is thus

$$\begin{aligned} V(\mathbf{r}) = & \sum_i V_i(\rho_i) + \sum_j V_j^{\text{eff}}(\rho_j) + \sum_{i,i'} V_{ii'}^{(3)}(\rho_i, \rho_{i'}, \rho_{ii'}) \\ & - (\pi/2A)C_{s2}/(z + a/\sqrt{2})^4 + V^{\text{ind}}(\mathbf{r}). \end{aligned} \quad (27)$$

The first term in Eq. (27) is a sum over (anisotropic) pair potentials for the surface layer, performed by integrating Eq. (11) using Gauss-rational quadrature.⁴⁴ For He-LiF, the anisotropy of the C_6 dispersion coefficients has no significant effect, but this may not be the case for other systems.

The second term is a sum over isotropic pair potentials for all ions *except* the surface layer, again performed using Steele's method. The calculated C_6 dispersion coefficients for bulk ions are scaled by the factor L , calculated from Eq. (20) to reproduce the correct limiting long-range behavior for He-LiF. The repulsion parameters and damping functions for bulk ions are taken to be the same as for surface ions, although for He-LiF their contribution is insignificant. The corrugation contribution from bulk ions is also negligible, although it was included in the present work.

The third term is a sum of Axilrod-Teller potentials for pairs of ions in the surface layer. Its surface-averaged component was evaluated by using Steele's method to sum over the index i , performing an explicit summation over i' for a 17×17 grid around each atom i . The sum must be performed separately for the cases where i and i' are the same or different types of ion. The use of Steele's method for the Axilrod-Teller term is an approximation, since the sum over i' varies slightly with the orientation of ρ_i in the

surface plane. However, since the three-body term is small, this approximation is adequate. The corrugation of the three-body term was not included, and no attempt was made to include repulsive three-body forces, higher-order terms in the three-body dispersion series, or damping of the many-body dispersion series.

The fourth term, involving the McLachlan C_{s2} coefficient, takes account of the modification of the dispersion forces involving the surface layer due to the presence of the bulk. As described above, the corresponding term involving C_{s1} vanishes when summed over the surface layer. The corrugation terms arising from the McLachlan terms are very small, and were not included.

The final term is the induction energy due to polarization of the adatom in the field of the lattice. This was evaluated as described by Steele,⁴¹ and its Fourier components are

$$V_{00}^{\text{ind}}(z) = -\alpha_{\text{He}} \left[\frac{8\pi}{A [1 + \exp(-\sqrt{2}\pi)]} \right]^2 \exp(-4\pi z/a), \quad (28)$$

$$V_{11}^{\text{ind}}(z) = \frac{1}{4} V_{00}^{\text{ind}}(z). \quad (29)$$

The coefficients C_6 , C_3 , ν , and C_{s2} needed in Eq. (27) may all be evaluated from $\alpha(i\omega)$ functions for the adatom and for the ions in the solid, using the Clausius-Mossotti equation for $\epsilon(i\omega)$ where necessary. The results obtained from the CHF values of $\alpha(i\omega)$ are listed in the first column of Table VII. It may be noted that the terms involving F^- are dominant for all the dispersion coefficients.

Two approaches to constructing a He-LiF potential based on the *ab initio* results may be envisaged. Either the CHF values may be used as they stand, complete with any systematic errors, or the physical insight gained from the *ab initio* calculations may be employed to estimate the true values of the parameters, together with reasonable estimates of additional parameters such as higher-order dispersion coefficients C_8 , C_{10} , etc. Both these approaches will be followed here, although only the latter may reasonably be expected to give agreement with experiment; it is nevertheless interesting to see how far a pure *ab initio* calculation, without correlation, can go in predicting the atom-surface potential.

It is known that CHF calculations underestimate the static polarizability of the bulk F^- ion by about 15%,¹² because of the lack of correlation, and it may be expected that the dispersion coefficients will be similarly underestimated. We have recently proposed a semiempirical model which allows the dispersion coefficients to be calculated from empirical ionic polarizabilities and rare-gas effective electron numbers;¹⁹ for He-LiF, this model yields $C_3 = 108 \text{ meV \AA}^3$. For atom-ion C_6 coefficients, the model consists simply of using the Slater-Kirkwood approximation, with the effective electron number for the ion taken to be the same as for the isoelectronic rare-gas atom.³⁷ The necessary static polarizabilities for surface ions were obtained by scaling the CHF values by the ratio required to bring the CHF and empirical values for bulk ions into agreement. C_8 coefficients were obtained from

C_6 coefficients assuming that the C_8/C_6 ratio was unchanged from the CHF value for bulk ions. The resulting dispersion coefficients are given in the second column of Table VII.

In the following discussion, two He-LiF potentials based on these calculations will be considered, both of the form of Eq. (27). The first, designated V^{CHF} , is defined by the CHF coefficients of Table VII, without any dispersion coefficients beyond C_8 . The second, designated V^{SE} , is defined by the semiempirical coefficients of Table VII, with higher-order dispersion coefficients up to C_{14} defined using the recursion relationships given in Eqs. (7), (8), and (9) of Ref. 45. For both potentials, the repulsive parts of the atom-ion potentials are given by the single exponential fits described in Tables I and II. The CHF potential has a well depth of 6.69 meV with the minimum at $z = 3.05 \text{ \AA}$, while the SE potential has a well depth of 8.11 meV with the minimum at $z = 2.98 \text{ \AA}$. The well depth required to reproduce the experimental bound-state energies¹⁶ is approximately 8.7 meV.

The different contributions to the surface-averaged component $V_{00}(z)$ of the SE potential are illustrated in Fig. 4. It may be seen that the potential in the region of the minimum is quite strongly dominated by the surface-layer sum; the contributions from the bulk and from the surface layer three-body term are of similar magnitude but opposite sign. The contribution from the McLachlan term is very small, and the induction contribution does not become important until $z < 2.5 \text{ \AA}$.

The Fourier components of the SE potential are compared with those of the potential of Celli, Eichenauer, Kaufhold, and Toennies¹⁰ (CEKT potential) in Fig. 5. It may be seen that the present potential is shifted to smaller z by about 0.06 \AA (because of the weaker SCF repulsion) and that the corrugation terms are significantly softer.

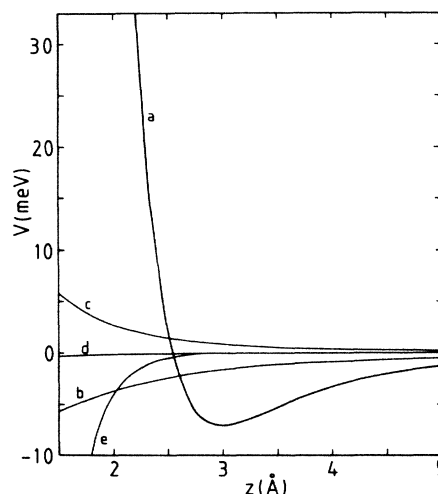


FIG. 4. Contributions to the surface-averaged component of the SE potential, $V_{00}(z)$. The contributions illustrated correspond to the successive terms in Eq. (27): curve *a*, pairwise sum over ions in the surface layer; curve *b*, pairwise sum over ions beneath the surface layer; curve *c*, Axilrod-Teller term summed over all pairs of ions in the surface layer; curve *d*, McLachlan substrate-mediated dispersion term; curve *e*, induction energy.

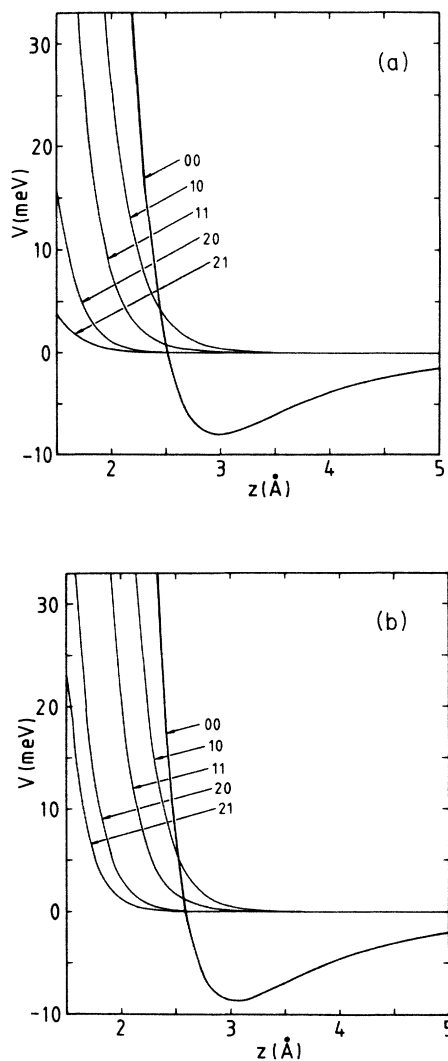


FIG. 5. Fourier components of the He-LiF potential: (a) SE potential (present work); (b) CEKT potential (Ref. 10).

The peak-to-peak corrugation of the SE potential is 0.53 Å at zero energy, decreasing to 0.46 Å at 100 meV; however, it should be noted that the peak-to-peak corrugation is quite strongly affected if the surface layers of Li^+ and F^- ions do not lie in the same plane. The well depth, by contrast, is only weakly influenced by such relaxation effects.

The bound states of the SE potential are compared with those of the CEKT potential and with the experimental values of Table VIII. The agreement for the present potential is of course poorer than for CEKT, since Celli *et al.* fitted to the bound-state energies and we did not. However, within the framework of the present model, it is possible to fit the bound states by making relatively small changes in the potential parameters, and without introducing unphysical long-range behavior as for the CEKT potential. Such a procedure requires detailed close-coupling calculations and comparisons with experimental diffractive scattering intensities, and is outside the scope of the present paper, but will be the subject of future work.

TABLE VIII. Comparison of calculated and experimental bound-state energies for He-LiF. Units of energy are meV.

	ν	CEKT ^a	SE	Experiment ^b
⁴ He	0	-5.95	-5.52	-5.90(6)
	1	-2.46	-2.15	-2.46(5)
	2	-0.86	-0.64	-0.78(4)
	3	-0.23	-0.13	-0.21(2)
³ He	0	-5.59	-5.18	-5.59(8)
	1	-1.96	-1.67	-2.00(6)

^aFrom Ref. 10.

^bFrom Ref. 16.

V. CONCLUSIONS

We have performed calculations of both the repulsive and the attractive parts of the He-LiF interaction potential, based on a pairwise-additive model of the interaction. Repulsion potentials involving ions in a crystalline environment were found to be considerably weaker than those involving free ions, because of the compression effects of the electrostatic field of the neighboring ions and the effects of overlap compression. Comparisons with first-order calculations of repulsion potentials show that the latter considerably overestimate the repulsion. Despite the fact that ions at a surface are in an anisotropic environment, the repulsion potential between a surface F^- ion and a He atom is not significantly anisotropic.

Dipole and quadrupole moments and static polarizabilities of surface F^- ions have been calculated, and compared with the corresponding properties of bulk and surface ions. The permanent moments of surface ions are too small to make a significant contribution to induction energies. Surface ions are a few percent more polarizable than bulk ions, but both are much less polarizable than free ions. This again reflects the compression of in-crystal ions by electrostatic and overlap effects.

Dispersion coefficients between He atoms and in-crystal (bulk and surface) ions have been calculated from coupled Hartree-Fock calculations, and show trends similar to those for static polarizabilities.

We have proposed a model for atom-surface interaction potentials involving ionic solids, based on pairwise additivity but including corrections for induction energy, nonadditive dispersion forces, and dielectric screening effects. Surface ions are treated differently from bulk ions, in that the pair potentials for surface ions have different dispersion coefficients from bulk ions, and may be anisotropic. The CHF values of the dispersion coefficients neglect intramolecular correlation effects, and are thus expected to be underestimates of the true coefficients. A semiempirical scheme was therefore used to estimate the true coefficients, using static polarizabilities scaled from the CHF results for ions in different environments. The resulting He-LiF atom-surface potential has a well depth of 8.11 meV, compared with an experimental value of approximately 8.7 meV.

There are various ways in which the present potential can be modified to bring the well depth into agreement with experiment. The calculated dispersion coefficients

may be in error by up to 10%, and such variations yield well depths which easily encompass the experimental value. There are also uncertainties in the form of the three-body potentials, and in the most appropriate way to damp the dispersion forces in atom-surface problems. The question of nonadditivity of the repulsive forces is also important, and has not yet been investigated. Future work will attempt to fit an interaction potential to molecular-beam scattering data for He-LiF, while still conforming to the theoretical constraints imposed by the present calculations.

Note added. A FORTRAN subroutine for evaluating the potentials proposed in the present paper is available on request from J.M.H. It performs the necessary summations, and returns the Fourier components of the atom-surface potential.

ACKNOWLEDGMENTS

The authors are grateful to Professor G. Scoles for stimulating their interest in the He-LiF problem, and to Dr. D. Eichenauer for sending them a copy of Ref. 10 before publication.

APPENDIX: SUMMATION OF THE McLACHLAN POTENTIAL OVER A LAYER OF SURFACE ATOMS

For the geometry shown in Fig. 3(b), McLachlan⁴³ gave an expression for the surface-mediated dispersion interaction

$$V_{\text{McL}}(\rho, \theta) = C_{s1} \frac{2 - 3 \cos(2\theta) - 3 \cos(2\theta')}{6(\rho\rho')^3} - \frac{C_{s2}}{(\rho')^6} \quad (\text{A1})$$

Substituting for ρ , ρ' , θ , and θ' in terms of z and t yields

$$V_{\text{McL}}(\rho, \theta) = \frac{C_{s1} \{4t^4 + [z^2 + (z+2d)^2]t^2 - 2z^2(z+2d)^2\}}{3\{(t^2+z^2)[t^2+(z+2d)^2]\}^{5/2}} - \frac{C_{s2}}{[t^2+(z+2d)^2]^3} \quad (\text{A2})$$

Steele's treatment⁴¹ now allows the summation over the surface layer to be transformed into an integral. For the surface-averaged potential, the integral of Eq. (11) becomes

$$V_{\text{McL}}^{00}(z) = (2\pi/A) \int_0^\infty V_{\text{McL}}(\rho, \theta) t dt \quad (\text{A3})$$

As may be verified by differentiation, the indefinite integral of this is

$$\frac{-C_{s1}t^2}{3\{(t^2+z^2)[t^2+(z+2d)^2]\}^{3/2}} + \frac{C_{s2}}{4[t^2+(z+2d)^2]^2} \quad (\text{A4})$$

The first term may be seen to vanish at both $t=0$ and $t=\infty$, and so makes no contribution to the surface-averaged potential. The second term makes a small attractive contribution given by

$$V_{\text{McL}}^{00}(z) = -(\pi/2A)C_{s2}/(z+2d)^4 \quad (\text{A5})$$

Klein *et al.*⁴⁶ have obtained the same result, but gave a rather different derivation.

*Present and permanent address: Department of Chemistry, University of Exeter, Stocker Road, Exeter, EX4 4QD, England.

¹T. H. Ellis, S. Iannotta, G. Scoles, and U. Valbusa, *Phys. Rev. B* **24**, 2307 (1981).

²J. M. Hutson and C. Schwartz, *J. Chem. Phys.* **79**, 5179 (1983).

³H. Jónsson, J. H. Weare, T. H. Ellis, G. Scoles, and U. Valbusa, *Phys. Rev. B* **30**, 4203 (1984).

⁴W. E. Carlos and M. W. Cole, *Surf. Sci.* **91**, 339 (1980).

⁵H. Jónsson and J. H. Weare, *Faraday Discuss. Chem. Soc.* (to be published).

⁶G. Vidali and M. W. Cole, *Phys. Rev. B* **29**, 6736 (1984).

⁷S. Chung, N. Holter, and M. W. Cole, *Phys. Rev. B* **31**, 6660 (1985).

⁸A. Tsuchida, *Surf. Sci.* **14**, 375 (1969).

⁹A. Tsuchida, *Surf. Sci.* **46**, 611 (1974).

¹⁰V. Celli, D. Eichenauer, A. Kaufhold, and J. P. Toennies, *J. Chem. Phys.* **83**, 2504 (1985).

¹¹G. D. Mahan, *Solid State Ionics* **1**, 29 (1980).

¹²P. W. Fowler and P. A. Madden, *Mol. Phys.* **49**, 913 (1983).

¹³K. T. Tang and J. P. Toennies, *J. Chem. Phys.* **80**, 3726 (1984).

¹⁴H.-J. Böhm and R. Ahlrichs (unpublished).

¹⁵A. Dalgarno and W. D. Davison, *Mol. Phys.* **13**, 479 (1967).

¹⁶G. Derry, D. Wesner, S. V. Krishnaswamy, and D. R. Frankl,

Surf. Sci. **74**, 245 (1978).

¹⁷L. W. Bruch and H. Watanabe, *Surf. Sci.* **65**, 619 (1977).

¹⁸R. J. Le Roy, *Surf. Sci.* **59**, 541 (1976).

¹⁹P. W. Fowler and J. M. Hutson, *Surf. Sci.* **165**, 289 (1986).

²⁰G. Brusdeylins, R. B. Doak, and J. P. Toennies, *Phys. Rev. B* **27**, 3662 (1983).

²¹G. Benedek, G. P. Brivio, L. Miglio, and V. R. Velasco, *Phys. Rev. B* **26**, 497 (1982).

²²P. W. Fowler and P. A. Madden, *Phys. Rev. B* **29**, 1035 (1984).

²³R. E. Watson, *Phys. Rev.* **111**, 1108 (1958).

²⁴P. W. Fowler and P. A. Madden, *J. Phys. Chem.* **89**, 2581 (1985).

²⁵E. A. Colbourn and W. C. Mackrodt, *Surf. Sci.* **117**, 571 (1982).

²⁶G. C. Benson and T. A. Claxton, *J. Chem. Phys.* **48**, 1356 (1968).

²⁷E. R. Cowley and J. A. Barker, *Phys. Rev. B* **28**, 3124 (1983).

²⁸F. B. van Duijneveldt, IBM Research Report No. RJ945, 1971 (unpublished).

²⁹S. F. Boys and F. Bernardi, *Mol. Phys.* **19**, 553 (1970).

³⁰The main part of the SCF point-charge induction energy is $-\frac{1}{2}\alpha F^2$, where α is the polarizability of the He atom and F is the field due to the point charge or point-charge lattice.

- However, there are also higher-order terms which depend upon the sign of the perturbing charge. The leading term of this type is $-\frac{1}{4}BF'F^2$, where B is the dipole-dipole-quadrupole hyperpolarizability [see A. D. Buckingham, *Adv. Chem. Phys.* **12**, 107 (1967)]. At the distances used in our calculations, this term contributes a few percent to the induction energy. Note that this term is relatively more important for the exponentially decaying field of a slab than for the Coulomb field of a single point charge.
- ³¹H.-J. Böhm and R. Ahlrichs, *J. Chem. Phys.* **77**, 2028 (1982).
³²L. Miglio, F. Quasso, and G. Benedek, *Surf. Sci.* **136**, L9 (1984).
³³L. Miglio, F. Quasso, and G. Benedek, *J. Chem. Phys.* **83**, 417 (1985).
³⁴R. M. Stevens, R. M. Pitzer, and W. N. Lipscomb, *J. Chem. Phys.* **38**, 550 (1963).
³⁵P. W. Fowler and N. C. Pyper (unpublished).
³⁶P. W. Fowler and P. A. Madden, *Phys. Rev. B* **30**, 6131 (1984).
³⁷P. W. Fowler, P. J. Knowles, and N. C. Pyper, *Mol. Phys.* **56**, 83 (1985).
³⁸R. D. Amos, N. C. Handy, P. J. Knowles, J. E. Rice, and A. J. Stone, *J. Phys. Chem.* **89**, 2186 (1985).
³⁹A. D. Buckingham, *Adv. Chem. Phys.* **12**, 107 (1967). Note that different definitions of the quadrupole moment and quadrupole polarizability are sometimes used. Some authors use $Q = 2\Theta$ and $\alpha_2 = 2C$.
⁴⁰G. Starkschall and R. G. Gordon, *J. Chem. Phys.* **56**, 2801 (1972).
⁴¹W. A. Steele, *The Interaction of Gases with Solid Surfaces* (Pergamon, Oxford, 1974).
⁴²E. M. Lifshitz, *Zh. Eksp. Teor. Fiz.* **29**, 94 (1955) [*Sov. Phys.—JETP* **2**, 73 (1956)].
⁴³A. D. McLachlan, *Mol. Phys.* **7**, 381 (1963).
⁴⁴Numerical Algorithms Group FORTRAN Library Manual, Mark 11, routines D01BBF and D01BAY (Numerical Algorithms Group, Oxford, 1984).
⁴⁵C. Douketis, G. Scoles, S. Marchetti, M. Zen, and A. J. Thakkar, *J. Chem. Phys.* **76**, 3057 (1982).
⁴⁶J. R. Klein, L. W. Bruch, and M. W. Cole (unpublished).